Available online at www.sciencedirect.com
ScienceDirect
Catalysis Today 132 (2008) 46–51
CATALYSIS TODAY
www.elsevier.com/locate/cattod

Characterization of acidic property of sulfo-group functionalized microporous and mesoporous silica by adsorption microcalorimetry

Fei-Yee Yeoh [a], Akihiko Matsumoto [a,*], Yoshiyuki Iwase [b], Toshihide Baba [b]

[a] *Department of Materials Science, Toyohashi University of Technology, 441-8122 Toyohashi, Japan*
[b] *Department of Environmental Chemistry and Engineering, Interdisciplinary Graduate School of Science and Engineering, Tokyo Institute of Technology, 226-8503 Yokohama, Japan*

Available online 1 February 2008

Abstract

Sulfo-group functionalized microporous and mesoporous silica based-on a MCM-41 framework which showed solid acid property were synthesized and characterized by adsorption microcalorimetry. Both the sulfo-functionalized microporous and mesoporous silica (Micro-SO_3H and Meso-SO_3H) were prepared by the oxidation of thiol group (–SH) included mesoporous silica which was obtained through the hydrolysis and co-condensation of tetramethoxysilane (TMOS) and mercaptopropyl trimethoxysilane (MPTMS). The samples have an ordered two-dimensional hexagonal pore array similar to that of MCM-41 as depicted from the XRD patterns. Nitrogen adsorption also shows that both microporous and mesoporous silica have pore characteristics similar to MCM-41, i.e. high surface area and high pore volume. However, pore regularity, surface area and pore volume decreased as the MPTMS loading increased. Solid-state ^{29}Si NMR indicated that the sulfo groups were successfully incorporated into both microporous and mesoporous silica frameworks. This sulfo-functionalized porous silica have high NH_3 uptakes and high differential heats of NH_3 adsorption, suggesting the presence of strong acidic sulfo groups on the silica surface. Acid catalyses of the samples were characterized by the isomerization reaction of but-1-ene to *cis*, *trans*-but-2-ene.

Keywords: Acid site; Adsorption microcalorimetry; Ammonia adsorption; Microporous silica; Mesoporous silica; Solid acids; Sulfo group

1. Introduction

Solid acids are important in many catalytic reactions [1–3]. Porous materials with high surface areas are good catalysts. However, many porous materials such as porous silica and porous carbon do not have strong acidic properties in nature. Thus, incorporation of acidic functional groups onto the surface of porous materials is a great challenge to obtain good solid acids [2,4–8]. MCM-41 is a well-known mesoporous silica with regular two-dimensional hexagonal structure [9–12]. The surface of MCM-41 has been chemically modified by various functional groups for different applications [13,14]. Research to incorporate metal and other functional groups to create Lewis and Brønsted acid sites in silica framework of MCM-41 have been reported [15–17]. Literature also show that the incorporation of strong acidic sulfo groups on ordered mesoporous silica such as MCM-41, SBA-15 and FSM-16 can efficiently catalyze various chemical reactions [18–29]. Pore size of a catalyst is one of the important features in selective adsorptions and reactions. Furthermore, in the case of adsorption in micropores, the adsorption is enhanced by overlapping interaction potential. In this study, synthesis and characterization of the sulfo-functionalized porous silica in both microporous and mesoporous ranges were attempted by the direct-hydrolysis and co-condensation of TMOS and MPTMS. The adsorption microcalorimetry of NH_3 and the catalytic activity of but-1-ene to *cis*, *trans*-but-2-ene of the samples were measured to elucidate the effect of pore size on the surface acidic property.

2. Experimental

2.1. Sample preparation

Sulfo-functionalized microporous and mesoporous silica were prepared in the same manner as reported [30,31]. The

* Corresponding author. Tel.: +81 532 446811; fax: +81 532 485833.
E-mail address: aki@tutms.tut.ac.jp (A. Matsumoto).

0920-5861/$ – see front matter © 2007 Elsevier B.V. All rights reserved.
doi:10.1016/j.cattod.2007.12.027

microporous silica included with sulfo groups were prepared as below. 3.08 g of decyltrimethylammonium bromide (C10TAB) was dissolved in 200 g mixed solution of water and methanol (300%, w/w). 4.32 ml of sodium hydroxide solution (NaOH aq., 1 M) was added to the surfactant solution as a basic catalyst. A mixture of 17.34 mmol tetramethoxysilane (TMOS) and mercaptopropyl trimethoxysilane (MPTMS) was then dropped into the basic surfactant solution to prepare a precursor gel of sulfo-functionalized microporous silica, namely Micro-SH-*n*%/C10TAB (where *n* is the molar percentage of MPTMS to total silica sources). The amount of thiol groups (–SH) was controlled by regulating the MPTMS amount. The mixture was then stirred at 298 K for 8 h. It was then filtered, washed and dried in an oven for 24 h. The as-synthesized sample was then refluxed in methanol for 24 h to extract the surfactant C10TAB. After surfactant removal, thiol-functionalized microporous silica was recovered and denoted as Micro-SH-*n*%. Finally, thiol groups on the surface of Micro-SH-*n*-% were oxidized into sulfo groups with a concentrated hydrogen peroxide solution (35% aq. H_2O_2) at room temperature to give sulfo-functionalized microporous silica, micro-SO_3H*n*%. As a control, microporous silica without any MPTMS loading (microporous MCM-41) was also synthesized and designated as micro-SH-0%.

The mesoporous silicas included with sulfo groups was prepared by a similar manner as micro-SO_3H-*n*%. 1.48 g of hexadecyltrymethylammonium bromide (C16TAB) was dissolved in 74 g of water–methanol mixed solution (methanol 30 mol%). A total of 1.3 mmol tetramethoxysilane (TMOS) and mercaptopropyl trimethoxysilane (MPTMS) mixture was then dripped in the surfactant solution. The amount of thiol groups was controlled from 0% to 30% by regulating the MPTMS amount. A precursor gel was formed when 8.2 g of tetramethylammonium hydroxide solution (TMAOH, 10%) was added into the mixture. The gel was stirred at room temperature and aged in a Teflon container at 368 K for 24 h. It was then filtered, washed and dried at 313 K for 15 h in an oven. The dried sample was designated as Meso-SH-*n*%/C16TAB (n = 10, 20 and 30 mol%). The template C16TAB was extracted in an ethanol and hydrochloric acid (9 mol%) mixed solution. After the surfactant removal, the thiol functionalized mesoporous silica was dried and designated as meso-SH-*n*%. Finally, meso-SH-*n*% was oxidized in a 35% hydrogen peroxide solution and denoted as meso-SO_3H-*n*%. Surfactant in meso-SH-0% (or mesoporous MCM-41) was removed by calcination at 823 K for 6 h as a control.

2.2. Characterizations

X-ray diffraction was measured by an automatic diffractometer (Rigaku RINT2000, Cu Kα). N_2 adsorption was measured volumetrically with an automatic adsorption apparatus (Quantachrome Autosorb I M) volumetrically at 77 K. A pretreatment was carried out at 383 K in 0.1 mPa for 11 h. Inclusion of sulfopropyl groups into silica framework was investigated with solid state ^{29}Si MAS-NMR with a 400 MHz spectrometer (Varian, VNMR400P).

2.3. NH_3 adsorption

Adsorption isotherm and differential heats of adsorption of NH_3 were measured simultaneously at 298 K by a volumetric adsorption apparatus attached with a twin-conduction type microcalorimeter (Tokyo Rico). Pretreatment was done at 383 K for 5 h in 0.1 mPa.

2.4. Catalytic activity

The catalyst (0.15 g) was packed in a continuous flow reactor (10 mm i.d. silica tubing) in a vertical furnace and heated under an N_2 stream at 0.15 K min^{-1} from room temperature to 423 K, and the sample was then heated at the same temperature for 1 h. After calcination of the catalyst, the reaction of but-1-ene was carried out using a continuous-flow reactor at atmospheric pressure. But-1-ene was fed with N_2 into the reactor via a mass flow meter. The partial pressure of but-1-ene and helium were 38 and 63 kPa, respectively. The contact time, W/F was 3.3 g h mol^{-1}, where W is the weight of the catalyst and F is a total feed rate (but-1-ene + He) (mol h^{-1}). Analyses for butenes, such as 2-methyl propene, and butanes were performed using Unicarbon A-400. The amounts of methane, ethane, propene and propane were determined using a Porapak Q column, and the amounts of hydrocarbons with more than three carbon atoms were determined using an OV-101 column.

3. Results and discussion

X-ray diffraction pattern of meso-SH-0% (Fig. 1) had a sharp peak at 2.4° and two smaller peaks at 4.1 and 4.8°, which were assigned to (1 0 0), (1 1 0) and (2 0 0) faces of *p6mm* structure of MCM-41 [10]. Meso-SH-*n*% showed a similar XRD pattern suggesting the retainment of regular pore structure. At a higher MPTMS loading, the intensity of the (1 0 0) peak was reduced and the high order peaks due to (1 1 0) and (2 0 0) faces were less obvious. XRD patterns of other micro-SH-*n*% showed similar patterns. The (1 0 0) peak was observed at 3.4° in the XRD pattern of Micro-SH-0%. Two

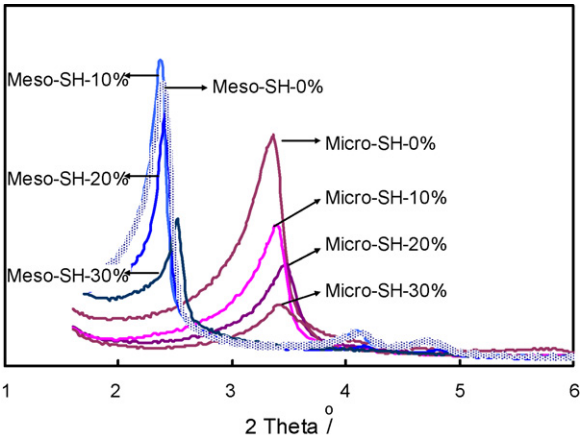

Fig. 1. XRD patterns of micro- and mesoporous silica with SH-0–30% after surfactant removal.

higher order peaks were found at 5.7° and 6.5°. The shift of peak positions from lower angle of meso-SH-*n*% to a higher angle of micro-SH-*n*% indicates a difference in the *d* spacing or size of unit cell. Presence of these XRD peaks indicates that the micro-SH-*n*% has an ordered structure as well as that of meso-SH-*n*%. The intensity of the (1 0 0) peak was reduced with increasing the amount of MPTMS loading for the mesoporous and the microporous samples, indicating a lower regularity of pore array by the perturbation effect of MPTMS [31,32].

Although XRD results show that both meso-SH-*n*% and micro-SH-*n*% have the same two-dimensional hexagonal structure of MCM-41, they exhibited different behaviors in N_2 adsorption (Fig. 2a). The adsorption isotherms of meso-SH-*n*% show a type IV character while those of micro-SH-*n*% showed a type I character [33,34]. Adsorption isotherms of meso-SH-*n*% showed a steep increase in adsorption uptake at the relative pressure (P/P_0) 0.1–0.4 due to capillary condensation in mesopores. This step shifted to a lower P/P_0 region for meso-SH-10%, -20% and -30% due to a smaller pore size by higher MPTMS loading. The step became less obvious with increasing MPTMS amount, especially for Meso-SH-30%, resulting from a broader pore size distribution. Adsorbed amount of meso-SH-*n*% and micro-SH-*n*% also decreased by increasing MPTMS amount. On the other hand, the type Ib isotherm of micro-SH-0% indicated microporosity in this sample (Fig. 2a). Combining with the XRD results, this phenomenon could be explained by the disruption of self-assembly of the surfactant and silica by introducing MPTMS during the synthesis, which eventually affects regularity of pore structure as well as pore characteristics, regardless of pore size.

After oxidation, the type IV adsorption isotherm was maintained for meso-SO_3H-10% (Fig. 2b) [33,34]. This indicates that the MCM-41 structure is well maintained after the addition of MPTMS and the oxidation of thiol groups on silica surface into sulfo groups by H_2O_2. As the MPTMS amount increases in the samples, the steep rise in adsorbed amount by capillary condensation became less obvious and the adsorbed amount became lower in meso-SO_3H-20% and -30%. A similar phenomenon was observed in the micro-SO_3H-*n*% series samples as well. The shape of the isotherm did not change after the oxidation, indicating the retainment of the pore structure. However, micro-SO_3H-20% showed a lower N_2 uptake compared to that of micro-SO_3H-10%. This depicted that oxidation by hydrogen peroxide led to partial collapse of the silica framework which might be due to hydrolysis. Samples with higher MPTMS loading were particularly weak against the hydrolysis by H_2O_2, because the amount of siloxane bridges in the structure decreases by increasing the amount of MPTMS.

Table 1
Pore characteristics of meso-SH-*n*%, micro-SH-*n*%, meso-SO_3H-*n*% and micro-SO_3H-*n*%

Samples	Surface area ($m^2\ g^{-1}$)	Pore size (nm)	Pore volume ($ml\ g^{-1}$)
Pore characteristics			
Meso-SH			
0%	950	3.5	0.66
10%	1040	3.2	0.62
20%	1280	2.9	0.59
30%	990	2.6	0.44
Meso-SO_3H			
10%	1020	3.5	0.67
20%	1060	2.9	0.47
30%	610	2.6	0.27
Micro-SH			
0%	1310	2.3	0.55
10%	810	1.6	0.37
20%	730	1.6	0.35
30%	490	1.6	0.23
Micro-SO_3H			
10%	730	1.6	0.34
20%	550	1.6	0.26
–	–	–	–

Pore characteristics of the samples estimated by adsorption of N_2 were summarized in Table 1. Meso-SH-0% and micro-SH-0% had high surface area and pore volume. Specific surface area of meso-SH-*n*% was retained around 1000 m^2/g. However, the surface area of micro-SH-*n*% decreased from 1310 to 490 m^2/g with the increase of MPTMS loading. This shows that the mesoporous silica with larger pore size is more stable compared to the microporous silica. The pore size distribution

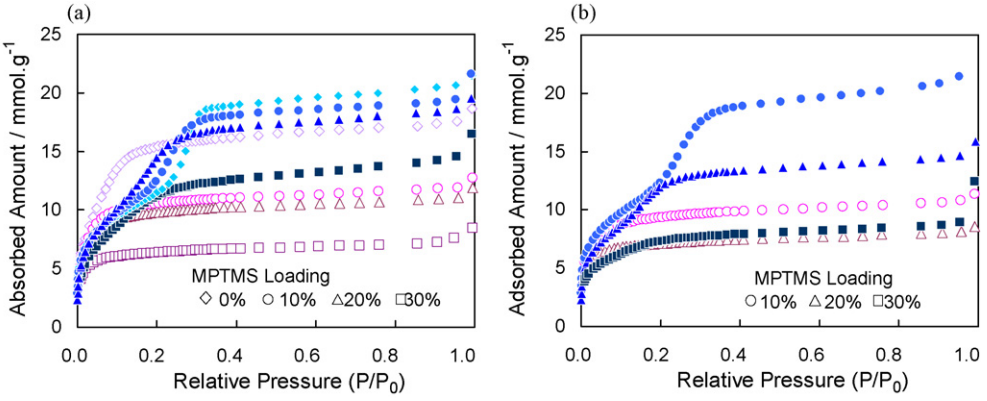

Fig. 2. Adsorption isotherms of N_2 on micro- and mesoporous samples (a) before oxidation (–SH-*n*%) and (b) after oxidation (–SO_3H-*n*%). Solid and blank symbols stand for mesoporous and microporous samples, respectively.

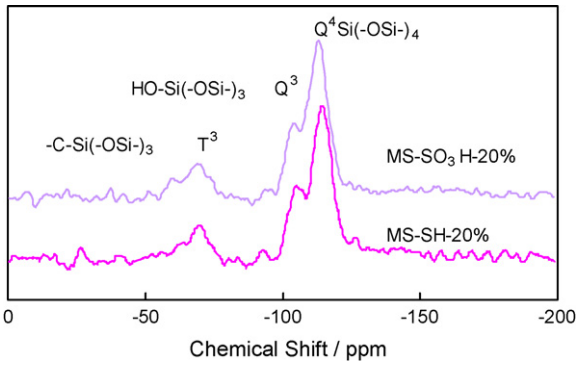

Fig. 3. ^{29}Si NMR spectra of mesoporous samples before (MS–SH-20%) and after oxidation (MS–SO_3H-20%).

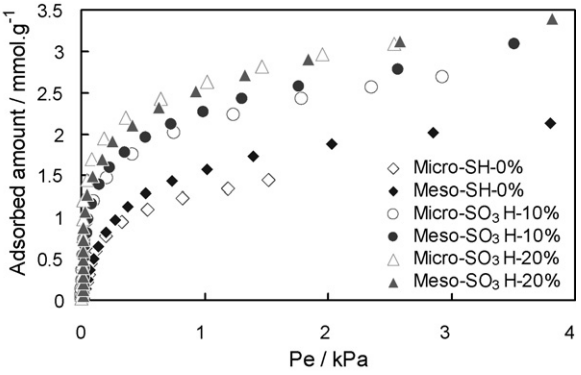

Fig. 5. Adsorption isotherm of ammonia for micro-0%, -10%, -20% and meso-0%, -10%, -20%.

was calculated by the DFT method, because this method provides a more accurate estimation on pore size across microporous and mesoporous regions compared to the conventional BJH method [35,36]. The pore size of meso-SH-*n*% systematically decrease from 3.5 to 2.6 nm with increased MPTMS loading. Micro-SH-*n*% showed a similar tendency: the pore size of micropore range decreased from 2.3 to 1.6 nm by inclusion of propylthiol. Pore volumes of both microporous and mesoporous samples decreased with the increase of MPTMS loading. After oxidation, both meso-SO_3H-*n*% and micro-SO_3H-*n*% showed a little decrease in surface area.

Solid state ^{29}Si NMR spectrum of meso-SH-20% (Fig. 3) showed two distinctive signals at −105 and −115 ppm which were assigned to silicon atoms at Q^3 [HOSi(OSi)$_3$] and Q^4 [Si(OSi)$_3$] environments, respectively. Besides the Q^3 and Q^4 signals, it also showed a T^3 signal at −68 ppm assigned to silicon positioned next to a methylene and three siloxane groups. The presence of methylene groups in the spectra has proven the incorporation of an organic functional group which contains carbon into the silica framework. Both meso-SH-20% and meso-SO_3H-20% showed similar spectra indicating the retainment of the functional group in the silica framework after oxidation. The NMR results for microporous samples showed a similar tendency [30]. Meso-SH-20% (Fig. 4) showed a few well-defined signals in ^{13}C NMR spectrum. Signals at 10, 22 and 27 ppm were respectively given by C1, C2 and C3 carbon atoms, in a propyl chain (Fig. 4) which bound a silicon atom (C1), two carbon atoms (C2), and a thiol group (C3) [25]. Another signal at 38 ppm attributed to a non-acidic disulfide group species. The sample showed a similar spectrum after oxidation with an absence of the C3 signal at 27 ppm, which was due to resonance of the carbon atom that bound to the thiol group. The C3 signal was replaced by a new C3′ signal at 54 ppm which was attributable to a methylene species positioned between a sulfo group and another methylene group. This indicates that the thiol group had been oxidized into the sulfo group. Both ^{29}Si and ^{13}C NMR had proven the incorporation of propylthiol group into the silica framework and the oxidation of the thiol group into the desired sulfo group.

The adsorption isotherm of NH_3 on meso-SO_3H-*n*% and micro-SO_3H-*n*% were shown in Fig. 5. Siliceous samples, meso-SH-0% and micro-SH-0%, were shown for comparison. The isotherm of each sample showed a type Ia character regardless of pore size, indicating a monolayer adsorption on the surface. Saturated NH_3 uptakes of the samples were calculated by the Langmuir equation. The saturated uptakes for micro-SO_3H-10% and meso-SO_3H-10% were 2.72 and 2.81 mmol/g, respectively, which were higher than those for micro-SH-0% (2.17 mmol/g) and meso-SH-0% (2.27 mmol/g). The higher adsorbed amounts in micro-SO_3H-10% and meso-SO_3H-10% were due to chemisorption of NH_3 on acidic sulfo

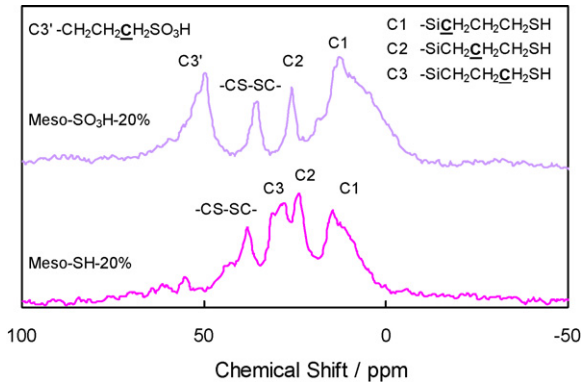

Fig. 4. ^{13}C NMR spectra of mesoporous samples before (MS–SH-20%) and after oxidation (MS–SO_3H-20%).

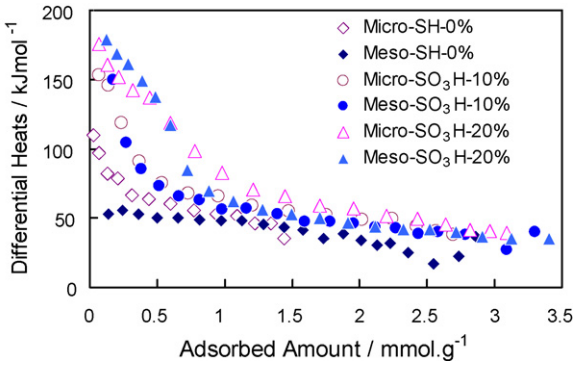

Fig. 6. Differential heat of ammonia adsorption for micro-SH-0%, micro-SO_3H-10%, -20% and meso-SH-0, meso-SO_3H-10%, -20%.

Table 2
Isomerization reaction of but-1-ene at 423 K

Sample	Conversion (%)	Products yield		Reaction rate (mmol g^{-1})
		cis-But-1-ene (%)	*trans*-But-1-ene (%)	
Meso-SH-0%	0	0	0	0
Meso-SO_3H-20%	19.1	51.1	48.9	1.9
Micro-SO_3H-20%	11.2	53.3	46.6	1.1

groups. Low adsorbed amounts of micro-SH-0% and meso-SH-0% indicated that only physical adsorption took place on the silica surfaces. As the MPTMS amount increased in the synthesis, the saturated NH_3 uptakes became even higher, i.e. 3.10 and 3.18 mmol/g for micro-SO_3H-20% and micro-SO_3H-20%, respectively. These results suggest that the adsorbed amount of NH_3 depends on the amount of sulfo group in the samples, which indicates that NH_3 would adsorb on an acidic sulfo group as discussed in later. Meso-SO_3H-*n*% gave higher saturated uptakes than micro-SO_3H-*n*% at the same sulfo concentration, *n*%, because of their higher surface areas.

The acidic characteristics of the porous samples were studied by adsorption microcalorimetry of NH_3. Fig. 6 shows the differential heats of adsorption of NH_3 on the prepared samples. The differential heat for meso-SH-0% was 50–40 kJ/mol at the initial stage of adsorption and slightly decreased with increasing the adsorption uptake. The heat would be due to physical adsorption of NH_3 on non-acidic sites since the physical adsorption gives rise to the differential heat lower than 70 kJ/mol [37]. On the other hand micro-SH-0% showed an adsorption heat of about 100 kJ/mol, slightly higher than that of meso-SH-0%, but the heat immediately decreased to about 50–60 kJ/mol. In the case of physical adsorption of vapor in micropores, the adsorption is enhanced by overlapping of the interaction potential from adjacent pore walls and adsorbate molecule strongly adsorbs in the pores [34]. The enhancement of adsorption potential was not exhibited by the adsorption isotherms, but by the adsorption microcalorimery. The higher initial heat for micro-SH-0% would be due to a stronger interaction between NH_3 and silica surface enhanced in micropores than meso-SH-0%.

On the other hand, the differential heat of adsorption on meso-SO_3H-10% was similar to that of micro-SO_3H-10%. The high initial heats ca. 150 kJ/mol were due to adsorption of NH_3 on acidic sites by chemisorption. The heats gradually decreased to 50–60 kJ/mol with increasing adsorption uptake until 0.8 mmol/g. The gradual decrease in adsorption heats indicated that the acid sites on the silica surface were rather heterogeneous. As the MPTMS loading was increased to 20 mol%, the initial heat became much higher, ca. 175 kJ/mol, in both meso-SO_3H-20% and micro-SO_3H-20%. The high heats evolution persisted longer to a higher adsorbed amount of ca. 1.0 mmol/g comparing to the cases of meso-SO_3H-10% and micro-SO_3H-10%. The higher heats were given by higher sulfo contents. Significant differences in the initial heats between meso-SO_3H-10% and micro-SO_3H-10% as well as between meso-SO_3H-20% and micro-SO_3H-20% were not observed regardless of the difference in pore sizes. It explains that the heat evolution by NH_3 chemisorption on acidic sulfo group is much greater compared to the heat evolution by overlapping the adsorption potential in micropores. Although the ^{13}C NMR spectra of the samples showed that almost all the thiol groups in meso-SH-20% have been oxidized into the sulfo groups, the amount of acidic sulfo groups estimated from the adsorption microcalorimetry were lower than the amount of the introduced thiol groups due to the formation of non-acidic disulfide groups (Fig. 4).

Acid catalytic behaviors of the samples were evaluated by the isomerization of but-1-ene to *cis*- and *trans*-2-butene. The results of acid catalytic behaviors of both meso-SO_3H-20% and micro-SO_3H-20% were shown in Table 2. The result of meso-SH-0% or siliceous MCM-41 was shown for comparison. Meso-SH-0% did not catalyze the reaction at all, despite good pore characteristics. It shows that the mesoporous silica does not exhibit an acidic catalytic behavior in this reaction without an acidic sulfo group. Meso-SO_3H-20% showed a relatively higher conversion rate (19%) with an equal product yield of *cis*-but-1-ene and *trans*-but-1-ene whilst micro-SO_3H-20% showed a lower conversion rate of 11.2%. These results indicate that the sulfo-incorporated samples exhibit an acid catalyst activity. The difference in conversion rate resulted from the difference in surface areas of the samples. After normalizing each sample by surface area, the conversion rate is almost identical for both samples, i.e. 0.018% and 0.020% for meso-SO_3H-20% and micro-SO_3H-20%, respectively.

4. Conclusions

Both sulfo-functionalized mesoporous and microporous silica were successfully prepared. These samples had a regular pore array with two-dimensional hexagonal structure same as MCM-41. Adsorption microcalorimetry of NH_3 showed that micro-SO_3H-*n*% and meso-SO_3H-*n*% had higher adsorption activities and differential heats of adsorption than that of micro-SH-0% and meso-SH-0% due to the chemisorption of NH_3 at acid sites, i.e. sulfo groups on silica surface. Micro-SO_3H-20% and meso-SO_3H-20% exhibited catalytic activity in the isomerization of but-1-ene in an acidic catalysis mechanism. Effect of the amounts of sulfo groups in the porous silica was more important than pore size in the chemisorption of NH_3.

Acknowledgements

Appreciations are due to ASEAN University Network/Southeast Asia Engineering Education Development Network (AUN/SEED-Net) and Japan International Cooperation Agency (JICA) for providing a doctoral scholarship of F.-Y. Yeoh.

References

[1] K. Tanabe, W.F. Hölderich, Appl. Catal. A 181 (1999) 399.
[2] M.A. Harmer, Q. Sun, Appl. Catal. A 221 (2001) 45.
[3] D. Ferri, S. Frauchiger, T. Bürgi, A. Baiker, J. Catal. 219 (2003) 425.
[4] N.K. Kala Raj, S.S. Deshpande, R.H. Ingle, T. Raja, P. Manikandan, Catal. Lett. 98 (2004) 217.
[5] E.F. Kozhevnikova, I.V. Kozhevnikov, J. Catal. 224 (2004) 164.
[6] M. Selvaraj, T.G. Lee, Micropor. Mesopor. Mater. 85 (2005) 39.
[7] D. Barreca, M.P. Copley, A.E. Graham, J.D. Holmes, M.A. Morris, R. Seraglia, T.R. Spalding, E. Tondello, Appl. Catal. A 304 (2006) 14.
[8] S.M. Mathew, A.V. Biradar, S.B. Umbarkar, M.K. Dongare, Catal. Commun. 7 (2006) 394.
[9] C.T. Kresge, M.E. Leonowicz, W.J. Roth, J.C. Vartuli, J.S. Beck, Nature 359 (1992) 710.
[10] J.S. Beck, J.C. Vartuli, W.J. Roth, M.E. Leonowicz, C.T. Kresge, K.D. Schmitt, C.T.-W. Chu, D.H. Olson, E.W. Sheppard, S.B. McCullen, J.B. Higgins, J.L. Schlenker, J. Am. Chem. Soc. 114 (1992) 834.
[11] U. Ciesla, F. Schüth, Micropor. Mesopor. Mater. 27 (1999) 131.
[12] C.T. Kresge, J.C. Vartuli, W.J. Roth, M.E. Leonowicz, in: O. Terasaki (Ed.), 1st ed., Studies in Surface Science and Catalysis, vol. 148, Elsevier, Amsterdam, 2004 , p. 53 (Chap. 4).
[13] O. Olkhovyk, M. Jaroniec, Adsorption 11 (2005) 685.
[14] A.M. Showkat, K.-P. Lee, A.I. Gopalan, M.-S. Kim, S.-H. Choi, H.-D. Kang, Polymer 46 (2005) 1804.
[15] A. Matsumoto, H. Chen, K. Tsutsumi, M. Grün, K. Unger, Micropor. Mesopor. Mater. 32 (1999) 55.
[16] S. Vetrivel, A. Pandurangan, J. Mol. Catal. A 227 (2005) 269.
[17] A.S. Dias, M. Pillinger, A.A. Valente, Micropor. Mesopor. Mater. 94 (2006) 214.
[18] I. Díaz, C. Márquez-Alvarez, F. Mohino, J. Pérez-Pariente, E. Sastre, J. Catal. 193 (2000) 283.
[19] I. Díaz, F. Mohino, J. Pérez-Pariente, E. Sastre, Appl. Catal. A 205 (2001) 19.
[20] I. Díaz, C. Márquez-Alvarez, F. Mohino, J. Pérez-Pariente, E. Sastre, Micropor. Mesopor. Mater. 44/45 (2001) 295.
[21] K. Wilson, A.F. Lee, D.J. Macquarrie, J.H. Clark, Appl. Catal. A 228 (2002) 127.
[22] J.S. Choi, D.J. Kim, S.H. Chang, W.S. Ahn, Appl. Catal. A 254 (2003) 225.
[23] I.K. Mbaraka, D.R. Radu, V.S.-Y. Lin, B.H. Shanks, J. Catal. 219 (2003) 329.
[24] D. Das, J.-F. Lee, S. Cheng, J. Catal. 223 (2004) 152.
[25] A.S. Dias, M. Pillinger, A.A. Valente, J. Catal. 229 (2005) 414.
[26] B. Karimi, M. Khalkhali, J. Mol. Catal. A 232 (2005) 113.
[27] B. Karimi, D. Zareyee, Tetrahedron Lett. 46 (2005) 4661.
[28] K. Shimizu, E. Hayashi, T. Hatamachi, T. Kodama, T. Higuchi, A. Satsuma, Y. Kitayama, J. Catal. 231 (2005) 131.
[29] B. Rác, M. Nagy, I. Pálinkó, A. Molnár, Appl. Catal. A 316 (2007) 152.
[30] A. Matsumoto, F.-Y. Yeoh, S. Fujihara, T. Baba, K. Tsutsumi, Adsorp. Sci. Technol. 24 (2006) 451.
[31] F.-Y. Yeoh, A. Matsumoto, Y. Iwase, T. Baba, Adsorp. Sci. Technol., in press.
[32] A.S.M. Chong, X.S. Zhao, A.T. Kustedjo, S.Z. Qiao, Micropor. Mesopor. Mater. 72 (2004) 33.
[33] K.S.W. Sing, D.H. Everett, R.A.W. Haul, L. Moscou, R.A. Oierotti, J. Rouquerol, T. Siemieniewska, Pure Appl. Chem. 57 (1985) 603.
[34] F. Rouquerol, J. Rouquerol, K. Sing, Adsorption by Powders and Porous Solids: Principles, Methodology and Applications, Academic Press, London, 1999 (Chapter 1).
[35] K.S.W. Sing, S.J. Gregg, Adsorption Surface Area and Porosity, Academic Press, London, 1982 (Chapter 4).
[36] P.I. Ravikovitch, A. Vishnyakov, R. Russo, A.V. Neimark, Langmuir 16 (2000) 2311.
[37] K. Tsutsumi, K. Nishimiya, Thermochim. Acta 143 (1989) 299.